

Design Equations for FRP– Strengthening of Columns

by **G. Monti and S. Alessandri**

Synopsis: The paper presents an analytical study on FRP–strengthened RC sections under combined bending and axial load. A secant approach is used that compares quite well with the exact one. As a result, closed-form equations are developed for designing in a straightforward way the amount of FRP needed to flexurally strengthen under–designed concrete columns.

Keywords: columns; FRP strengthening; interaction domain; seismic upgrade

1068 Monti and Alessandri

Giorgio Monti is a Full Professor of Structural Engineering at the University “La Sapienza” of Rome. He is member of the Commission Design of *fib* (fédération internationale du béton), in the groups “Seismic Concrete Design”, “Computer-based Modelling and Design” and “Design of Structures Reinforced by FRP”. His research interests span from reliability to the assessment and retrofitting of existing structures in seismic zones.

Silvia Alessandri is a PhD student in Structural Engineering at the Università La Sapienza of Rome. Her research interests concern FRP-strengthening of reinforced concrete structures, finite element modelling, and experimental behaviour of reinforced concrete members.

INTRODUCTION

When assessing the seismic performance of existing reinforced concrete buildings designed according to obsolete codes, one can identify potentially dangerous situations that could result in catastrophic failures. Among these, a typical inadequacy lies in the so-called “strong beam-weak column” situation, which, if extended to all columns at a given floor, can lead to the development of soft-storey mechanisms.

Such weaknesses should be eliminated by upgrading all weak columns in the zones of potential formation of plastic hinges. By no means should one pursue in these zones a ductility increase, which can result in unfavorable P–delta effects. Instead, one should aim at increasing the flexural capacity of those zones, with the objective of relocating the potential plastic hinges from the columns to the beams, thus re-establishing a desirable “weak beam-strong column” situation. This can be achieved by strengthening the column end sections so that, at a given beam-column joint, the sum of the column flexural capacities becomes larger than the sum of the framing beam capacities.

A possible way to obtain this behavior is to apply FRP sheets along the column faces, with the fibers oriented parallel to the column axis, at the end zones. From the technological standpoint, this solution requires to conceive appropriate devices to fasten the FRP sheet ends to the beams soffit, so that they can contribute their full strength at the critical column section, without debonding.

Once this practical aspect is solved, the problem remains of determining the adequate amount of FRP-strengthening to be applied to the column sections in order to obtain the sought flexural capacities.

As a matter of fact, design equations for FRP-strengthening have been easily derived for beams, under pure bending, and, after having been the object of countless experimental studies worldwide, are now incorporated in most recent codes or instructions. On the other hand, to the authors’ knowledge, no such equation has been proposed so far for the case of columns, where, apparently, the interaction with the axial load has represented a serious obstacle to the development of a simple and practical formulation.

Having said this, it should be clear that the intent of this paper is to propose a possible solution to this need: find a simple procedure that possibly makes use of closed-form equations, to design the correct amount of FRP strengthening in a column, with due consideration of the interaction with the axial load. Also, as a byproduct of this study, it would be expedient to relate the amount of FRP strengthening to the resultant failure mode and, possibly, to determine a set of limitations for it.

This is done by first presenting the classic treatment for unstrengthened column sections, with the purpose of introducing the notation of the non-dimensional approach and to describe the failure modes considered. Then, the equations are extended to the case of FRP-strengthened column sections, after which, the quite cumbersome “exact” approach followed so far is made more accessible and usable by simplification of the equations through a secant approach. This produces a segmentation of the “bending moment–axial load” interaction domain that compares to the exact one reasonably well. The summary of the procedure concludes the paper.

UNSTRENGTHENED SECTIONS UNDER COMBINED BENDING AND AXIAL LOAD

Reinforced concrete section analysis at the ultimate limit state under combined bending and axial is based on the following usual hypotheses:

- plane sections remain plane (linear strains);
- perfect bond between steel and concrete;
- no tensile strength in concrete;
- non-linear stress-strain laws for steel (bilinear) and concrete (parabola-rectangle).

The strain state over the section is uniquely defined by the concrete compression strain ε_c and by the steel tensile strain ε_s . Flexural failure occurs when one of the following conditions is met: $\varepsilon_c = \varepsilon_{cu} = 0.0035$, the concrete ultimate strain, or $\varepsilon_s = \varepsilon_{su} = 0.01$, the steel ultimate strain. Referring to the representation in

Figure 1, sectional failure can occur in one of the following modes ($\varepsilon_{yd} = 0.002 =$ yield strain):

- $\varepsilon_c < \varepsilon_{cu}$ and $\varepsilon_s = \varepsilon_{su}$ (mode 1);
- $\varepsilon_c = \varepsilon_{cu}$ and $\varepsilon_{yd} \leq \varepsilon_s < \varepsilon_{su}$ (mode 2);
- $\varepsilon_c = \varepsilon_{cu}$ and $0 \leq \varepsilon_s < \varepsilon_{yd}$ (mode 3).

Exact approach

Consider a rectangular cross-section with different top and bottom reinforcement, under combined bending and axial load. The non-dimensional equilibrium equations (translation and rotation) can be written as follows:

$$\alpha \xi + \mu_s (s' u - s) = n_{sd} \quad (1)$$

$$\alpha \xi [0.5(1 + \delta) - k \xi] + 0.5 \mu_s (1 - \delta)(s' u + s) = m_{Rd} \quad (2)$$

1070 Monti and Alessandri

where $n_{Sd} = \frac{N_{Sd}}{bd0.85f_{cd}}$ and $m_{Rd} = \frac{M_{Rd}}{bd^20.85f_{cd}}$ are the non-dimensional values of the

applied axial load N_{Sd} , and of the resisting moment M_{Rd} , respectively, where b = section width, d = section depth and f_{cd} = design concrete compressive strength (0.85 accounts for long-term loads). The coefficient α defines the equivalent stress block; its value depends on the concrete compression strain ε_c . The non-dimensional parameter $\xi = x/d$ defines the neutral axis depth; k is the concrete compression resultant depth; $\delta = d'/d$ is the cover ratio, where d' is its thickness; $u = A'_s/A_s$ is the top/bottom reinforcement ratio, while s and s' are the steel stress ratios: $s' = \sigma'_s/f_{yd}$ e $s = \sigma_s/f_{yd}$.

The ratio $\mu_s = \frac{A_s \cdot f_{yd}}{0.85 \cdot f_{cd} \cdot b \cdot d}$ represents the tensile steel reinforcement mechanical ratio.

With the only exception of mode 2, where it is directly computed, in all modes the non-dimensional neutral axis depth ξ should be determined by iteratively solving Equation 1.

Approximate (secant) approach

In order to avoid such iterative approach, it is possible, through the secant method, to find simplified expressions for the resisting moment as function of the acting axial load. Mode 1 is usually subdivided into two sub-modes: mode 1a and mode 1b, which differ in the compression steel state, either elastic or yielded.

Mode 1a — It is defined by: $\varepsilon_s = \varepsilon_{su}$, $\varepsilon_c < \varepsilon_{cu}$, $\varepsilon'_s \leq \varepsilon_{yd}$; the limiting conditions are: $\varepsilon_c = 0$ and $\varepsilon'_s = \varepsilon_{yd}$. Stress ratios are: $-5\delta \leq s' \leq 1$, $s = 1$. The neutral axis depth varies between the boundaries: $\xi = 0$, for $\varepsilon_c = 0$, and $\xi = \frac{1+5\delta}{6}$, for $\varepsilon'_s = \varepsilon_{yd}$.

The corresponding non-dimensional axial load varies between the boundaries:

$$n_{d0} = -\mu_s(1+5\delta u), \text{ for } \varepsilon_c = 0 \quad (3)$$

and, recalling that $\alpha \cong 2/3$:

$$n_{d1} = \frac{(1+5\delta)}{9} + \mu_s(u-1), \text{ for } \varepsilon'_s = \varepsilon_{yd} \quad (4)$$

The non-dimensional resisting moment varies between the boundaries:

$$m_{Rd0} = 0.5\mu_s(1-5\delta u)(1-\delta), \text{ for } \varepsilon_c = 0 \quad (5)$$

and, recalling that, for $\varepsilon'_s = \varepsilon_{yd}$, one has $k \cong 1/3$, thus:

$$m_{Rd1} = \frac{(1+5\delta)}{18} \left[(1+\delta) - \frac{(1+5\delta)}{9} \right] + \mu_s(1-\delta)(u+1), \text{ for } \varepsilon'_s = \varepsilon_{yd} \quad (6)$$

Through the secant method and assuming a typical value of $\delta = 0.05$, the equation of the resisting moment for mode 1a is given by:

$$m_{Rd(1a)}(n_d) \cong 0.475\mu_s(1-0.25u) + \frac{1}{2} \frac{1.2+12\mu_s u}{1.4+12\mu_s u} [n_d + \mu_s(1+0.25u)] \quad (7)$$

with the axial load varying between: $n_{d0} = -\mu_s(1+0.25u)$ and $n_{d1} = 0.14 + \mu_s(u-1)$

Mode 1b — It is defined by: $\varepsilon_s = \varepsilon_{su}$, $\varepsilon_c \leq \varepsilon_{cu}$, $\varepsilon'_s \geq \varepsilon_{yd}$; the limiting conditions are: $\varepsilon'_s = \varepsilon_{yd}$ and $\varepsilon_c = \varepsilon_{cu}$. Stress ratios are: $s'=1$, $s=1$. The neutral axis depth varies between the boundaries: $\xi = \frac{1+5\delta}{6}$, for $\varepsilon'_s = \varepsilon_{yd}$, and $\xi = 0.259$, for $\varepsilon_c = \varepsilon_{cu}$.

The corresponding non-dimensional axial load varies between the boundaries:

$$n_{d1} = \frac{(1+5\delta)}{9} + \mu_s(u-1), \text{ for } \varepsilon'_s = \varepsilon_{yd} \quad (8)$$

recalling that $\alpha \cong 2/3$, and, recalling that $\alpha \cong 0.8$:

$$n_{d2} = 0.2 + \mu_s(u-1), \text{ for } \varepsilon_c = \varepsilon_{cu} \quad (9)$$

By assuming α constant and $\cong 0.8$, the neutral axis depth is known:

$$\xi = \frac{n_{Sd} - \mu_s(u-1)}{\alpha} = \frac{n_{Sd} - \mu_s(u-1)}{0.8} \quad (10)$$

and the resisting moment equation is:

$$m_{Rd(1b)}(n_{Sd}) = \frac{1}{2} [n_{Sd} - \mu_s(u-1)] [(1+\delta) - n_{Sd} + \mu_s(u-1)] + 0.5\mu_s(1-\delta)(u+1) \quad (11)$$

By assuming a typical value of $\delta = 0.05$, the equation of the resisting moment for mode 1b is given by:

$$m_{Rd(1b)}(n_{Sd}) \cong \frac{1}{2} [n_{Sd} - \mu_s(u-1)] [1.05 - n_{Sd} + \mu_s(u-1)] + 0.475\mu_s(u+1) \quad (12)$$

Mode 2 — It is defined by: $\varepsilon_{su} \leq \varepsilon_s \leq \varepsilon_{yd}$, $\varepsilon_c = \varepsilon_{cu}$, $\varepsilon'_s \geq \varepsilon_{yd}$; the limiting conditions are: $\varepsilon_s = \varepsilon_{su}$ and $\varepsilon_s = \varepsilon_{yd}$. Stress ratios are: $s'=1$, $s=1$. The neutral axis depth varies between the boundaries: $\xi = 0.259$, for $\varepsilon_s = \varepsilon_{su}$, and $\xi = 0.636$, for $\varepsilon_s = \varepsilon_{yd}$.

The corresponding non-dimensional axial load varies between the boundaries:

1072 Monti and Alessandri

$$n_{d2} = 0.2 + \mu_s(u-1), \text{ for } \varepsilon_s = \varepsilon_{su} \quad (13)$$

Recalling that $\alpha \cong 0.8$, and:

$$n_{d3} = 0.51 + \mu_s(u-1), \text{ for } \varepsilon_s = \varepsilon_{yd} \quad (14)$$

The neutral axis depth is known:

$$\xi = \frac{n_{Sd} - \mu_s(u-1)}{\alpha} = \frac{n_{Sd} - \mu_s(u-1)}{0.8} \quad (15)$$

By assuming a typical value of $\delta = 0.05$, the equation of the resisting moment for mode 2 is given by:

$$m_{Rd(2)}(n_{Sd}) \cong \frac{1}{2} [n_{Sd} - \mu_s(u-1)] [1.05 - n_{Sd} + \mu_s(u-1)] + 0.475 \mu_s(u+1) \quad (16)$$

Mode 3 — It is defined by: $\varepsilon_{yd} \leq \varepsilon_s \leq 0$, $\varepsilon_c = \varepsilon_{cu}$, $\varepsilon'_s \geq \varepsilon_{yd}$; the limiting conditions are: $\varepsilon_s = \varepsilon_{yd}$ and $\varepsilon_s = 0$. Stress ratios are: $s'=1$, $1 \geq s \geq 0$. The neutral axis depth varies between the boundaries: $\xi = 0.636$, for $\varepsilon_s = \varepsilon_{yd}$, and $\xi = 1$, for $\varepsilon_s = 0$.

The corresponding non-dimensional axial load varies between the boundaries:

$$n_{d3} = 0.51 + \mu_s(u-1), \text{ for } \varepsilon_s = \varepsilon_{yd} \quad (17)$$

recalling that $\alpha \cong 0.8$, and:

$$n_{d4} = 0.8 + \mu_s u, \text{ for } \varepsilon_s = 0 \quad (18)$$

The non-dimensional resisting moment varies between the boundaries:

$$m_{Rd3} = 0.51 [0.5(1+\delta) - 0.26] + 0.5 \mu_s (1-\delta)(u+1), \text{ for } \varepsilon_s = \varepsilon_{yd} \quad (19)$$

recalling that $k \cong 0.4$ and:

$$m_{Rd4} = 0.8 [0.5(1+\delta) - 0.4] + 0.5 \mu_s (1-\delta)u, \text{ for } \varepsilon_s = 0 \quad (20)$$

Through the secant method and assuming a typical value of $\delta = 0.05$, the equation of the resisting moment for mode 3 is given by:

$$m_{Rd(3)}(n_{Sd}) \cong 0.14 + 0.475 \mu_s(u+1) - \frac{1+10\mu_s}{7+20\mu_s} [n_{Sd} - 0.51 - \mu_s(u-1)] \quad (21)$$

with the axial load varying between: $n_{d3} = 0.51 + \mu_s(u-1)$ and $n_{d4} = 0.8 + \mu_s u$.

Comparison between exact and approximate approaches

In Figure 2 a comparison is shown between the interaction diagram obtained through the exact approach and that obtained through the approximate (secant) approach. It is noted that the comparison is satisfactory and that the maximum error committed is

about 10%. However, the portions on the diagram of main interest for design purposes, that is, those pertaining to modes 1a, 1b and 2, are accurately represented, with errors as low as 5%.

FRP-STRENGTHENED SECTIONS UNDER COMBINED BENDING AND AXIAL LOAD

FRP-strengthening of sections under combined bending and axial load can be pursued through the application on the column sides of one or more layers of fabric. FRP-strengthened RC section analysis at the ultimate limit state is based on the same usual hypotheses adopted for the unstrengthened section, with the addition of the following:

- perfect bond between FRP and concrete;
- no compressive strength in FRP;
- linear stress-strain law for FRP.

The strain state over the section is uniquely defined by the concrete compression strain ε_c and by the FRP tensile strain ε_f . Flexural failure occurs when one of the following conditions is met: $\varepsilon_c = \varepsilon_{cu} = 0.0035$, the concrete ultimate strain, or $\varepsilon_f = \varepsilon_{fd}$, the FRP ultimate strain (usually, debonding). For this latter it is assumed, with any loss of generality, that, when $\varepsilon_f = \varepsilon_{fd}$, steel has yielded, *i.e.*, $\varepsilon_{yd} \leq \varepsilon_s \leq \varepsilon_{su}$ ($\varepsilon_{yd} = 0.002$, $\varepsilon_{su} = 0.01$ are the steel yield and ultimate strain, respectively).

Referring to the representation in

Figure 3, sectional failure can occur in one of the following modes:

- $\varepsilon_c < \varepsilon_{cu}$ and $\varepsilon_f = \varepsilon_{fd}$ (mode 1);
- $\varepsilon_c = \varepsilon_{cu}$ and $\varepsilon_{yd} \leq \varepsilon_f < \varepsilon_{fd}$ (mode 2).

Exact approach

Consider a rectangular cross-section with different top and bottom reinforcement and with FRP strengthening at the bottom, under combined bending and axial load. The non-dimensional equilibrium equations (translation and rotation) can be written as follows:

$$\alpha \xi + \mu_s (s' u - s) - \mu_f s_f = n_{sd} \quad (22)$$

$$\alpha \xi [0.5(1 + \delta) - k\xi] + 0.5 \mu_s (1 - \delta)(s' u + s) + 0.5 \mu_f s_f (1 + \delta) = m_{rd} \quad (23)$$

with the same definitions as for the case of unstrengthened section, and where the ratio

$\mu_f = \frac{A_f \cdot f_{fd}}{0.85 \cdot f_{cd} \cdot b \cdot d}$ represents the FRP-strengthening mechanical ratio, where A_f = FRP area, and f_{fd} = debonding strength; s_f = FRP stress ratio, given by:

$$s_f = \sigma_f / f_{fd} \quad (24)$$

In all modes the non-dimensional neutral axis depth ξ should be determined by iteratively solving Equation 22.

1074 Monti and Alessandri

Approximate (secant) approach

Also in this case, in order to avoid such iterative approach, it is possible, through the secant method, to find simplified expressions for the resisting moment as function of the acting axial load.

Mode 1 is also subdivided into two sub-modes: mode 1a and mode 1b, which differ in the compression steel state, either elastic or yielded.

Mode 1a — It is defined by: $\varepsilon_f = \varepsilon_{fd}$, $\varepsilon_c < \varepsilon_{cu}$; the limiting conditions are: $\varepsilon_c = 0$ and $\varepsilon'_s = \varepsilon_{yd}$. Stress ratios are: $-\frac{\varepsilon_{fd}}{\varepsilon_{yd}} \frac{\delta}{1+\delta} \leq s' \leq 1$, $s = 1$, $s_f = 1$. The neutral axis depth varies between the boundaries: $\xi = 0$, for $\varepsilon_c = 0$, and $\xi = \frac{\varepsilon_{yd}(1+\delta) + \varepsilon_{fd}\delta}{\varepsilon_{yd} + \varepsilon_{fd}}$, for $\varepsilon'_s = \varepsilon_{yd}$.

The corresponding non-dimensional axial load varies between the boundaries:

$$n_{d0} = -\mu_s \left(\frac{\varepsilon_{fd}}{\varepsilon_{yd}} \frac{\delta}{1+\delta} u + 1 \right) - \mu_f, \text{ for } \varepsilon_c = 0 \quad (25)$$

and, recalling that $\alpha \cong 2/3$:

$$n_{d1} = \frac{2}{3} \frac{\varepsilon_{yd}(1+\delta) + \varepsilon_{fd}\delta}{\varepsilon_{yd} + \varepsilon_{fd}} + \mu_s (u-1) - \mu_f, \text{ for } \varepsilon'_s = \varepsilon_{yd} \quad (26)$$

The non-dimensional resisting moment varies between the boundaries:

$$m_{Rd0} = 0.5\mu_s (1-\delta) \left(1 - \frac{\varepsilon_{fd}}{\varepsilon_{yd}} \frac{\delta}{1+\delta} u \right) + 0.5\mu_f (1+\delta), \text{ for } \varepsilon_c = 0 \quad (27)$$

and, recalling that, for $\varepsilon'_s = \varepsilon_{yd}$, one has $k \cong 1/3$:

$$m_{Rd1} = \frac{2}{3} \frac{\varepsilon_{yd}(1+\delta) + \varepsilon_{fd}\delta}{\varepsilon_{yd} + \varepsilon_{fd}} \left[0.5(1+\delta) - \frac{1}{3} \frac{\varepsilon_{yd}(1+\delta) + \varepsilon_{fd}\delta}{\varepsilon_{yd} + \varepsilon_{fd}} \right] + 0.5\mu_s (1-\delta)(u+1) + 0.5\mu_f (1+\delta) \quad (28)$$

In order to simplify the above equations, one can assume, without loss of accuracy, $\delta = 0$. Introducing the variable:

$$\xi_{s1} = \frac{\varepsilon_{yd}}{\varepsilon_{yd} + \varepsilon_{fd}} = \frac{2}{2 + 1000\varepsilon_{fd}} = \frac{r}{r+1} \quad (29)$$

where:

$$r = \frac{2}{1000\varepsilon_{fd}} \quad (30)$$

the axial load varies between the boundaries:

$$n_{d0} = -(\mu_s + \mu_f), \text{ for } \varepsilon_c = 0 \quad (31)$$

and

$$n_{d1} = \frac{2}{3}\xi_1 + \mu_s(u-1) - \mu_f, \text{ for } \varepsilon'_s = \varepsilon_{yd} \quad (32)$$

The non-dimensional resisting moment varies between the boundaries:

$$m_{Rd0} \cong \frac{1}{2}(\mu_s + \mu_f), \text{ for } \varepsilon_c = 0 \quad (33)$$

and

$$m_{Rd1} \cong \frac{2}{3}\xi_1 \left[\frac{1}{2} - \frac{1}{3}\xi_1 \right] + \frac{1}{2}\mu_s(u+1) + \frac{1}{2}\mu_f, \text{ for } \varepsilon'_s = \varepsilon_{yd} \quad (34)$$

Mode 1b — It is defined by: $\varepsilon_f = \varepsilon_{fd}$, $\varepsilon_c \leq \varepsilon_{cu}$, $\varepsilon'_s \geq \varepsilon_{yd}$; the limiting conditions are: $\varepsilon'_s = \varepsilon_{yd}$ and $\varepsilon_c = \varepsilon_{cu}$. Stress ratios are: $s'=1$, $s=1$, $s_f=1$. The neutral axis depth varies between the boundaries: $\xi = \frac{\varepsilon_{yd}(1+\delta) + \varepsilon_{fd}\delta}{\varepsilon_{yd} + \varepsilon_{fd}}$, for $\varepsilon'_s = \varepsilon_{yd}$, and $\xi = \frac{\varepsilon_{cu}(1+\delta)}{\varepsilon_{cu} + \varepsilon_{fd}}$,

for $\varepsilon_c = \varepsilon_{cu}$.

The corresponding non-dimensional axial load varies between the boundaries:

$$n_{d1} = \frac{2}{3} \frac{\varepsilon_{yd}(1+\delta) + \varepsilon_{fd}\delta}{\varepsilon_{yd} + \varepsilon_{fd}} + \mu_s(u-1) - \mu_f, \text{ for } \varepsilon'_s = \varepsilon_{yd} \quad (35)$$

Recalling that $\alpha \cong 2/3$, and, recalling that $\alpha \cong 0.8$:

$$n_{d2} = 0.8 \frac{\varepsilon_{cu}(1+\delta)}{\varepsilon_{cu} + \varepsilon_{fd}} + \mu_s(u-1) - \mu_f, \text{ for } \varepsilon_c = \varepsilon_{cu} \quad (36)$$

The non-dimensional resisting moment varies between the boundaries:

$$m_{Rd1} = \frac{2}{3} \frac{\varepsilon_{yd}(1+\delta) + \varepsilon_{fd}\delta}{\varepsilon_{yd} + \varepsilon_{fd}} \left[0.5(1+\delta) - \frac{1}{3} \frac{\varepsilon_{yd}(1+\delta) + \varepsilon_{fd}\delta}{\varepsilon_{yd} + \varepsilon_{fd}} \right] + \quad (37)$$

$$+ 0.5\mu_s(1-\delta)(u+1) + 0.5\mu_f(1+\delta)$$

and, recalling that, for $\varepsilon_c = \varepsilon_{cu}$, one has $k \cong 0.4$, thus:

1076 Monti and Alessandri

$$m_{Rd2} = 0.8 \frac{\varepsilon_{cu}(1+\delta)}{\varepsilon_{cu} + \varepsilon_{fd}} \left[0.5(1+\delta) - 0.4 \frac{\varepsilon_{cu}(1+\delta)}{\varepsilon_{cu} + \varepsilon_{fd}} \right] + 0.5\mu_s(1-\delta)(u+1) + 0.5\mu_f(1+\delta), \text{ for } \varepsilon_c = \varepsilon_{cu} \quad (38)$$

Assuming $\delta = 0$ and introducing the variable:

$$\xi_2 = \frac{\varepsilon_{cu}}{\varepsilon_{cu} + \varepsilon_{fd}} = \frac{3.5}{3.5 + 1000\varepsilon_{fd}} = \frac{1.75 \cdot r}{1.75 \cdot r + 1} \quad (39)$$

the axial load varies between the boundaries:

$$n_{d1} = \frac{2}{3}\xi_1 + \mu_s(u-1) - \mu_f, \text{ for } \varepsilon'_s = \varepsilon_{yd} \quad (40)$$

$$n_{d2} = 0.8\xi_2 + \mu_s(u-1) - \mu_f, \text{ for } \varepsilon_c = \varepsilon_{cu} \quad (41)$$

The non-dimensional resisting moment varies between the boundaries:

$$m_{Rd1} \cong \frac{2}{3}\xi_1 \left[\frac{1}{2} - \frac{1}{3}\xi_1 \right] + \frac{1}{2}\mu_s(u+1) + \frac{1}{2}\mu_f, \text{ for } \varepsilon'_s = \varepsilon_{yd} \quad (42)$$

$$m_{Rd2} \cong 0.8\xi_2 \left[\frac{1}{2} - 0.4\xi_2 \right] + \frac{1}{2}\mu_s(u+1) + \frac{1}{2}\mu_f, \text{ for } \varepsilon_c = \varepsilon_{cu} \quad (43)$$

Mode 2 — It is defined by: $\varepsilon_{fd} \leq \varepsilon_f \leq \varepsilon_{yd} \frac{0.36+\delta}{0.36}$, $\varepsilon_c = \varepsilon_{cu}$, $\varepsilon'_s \geq \varepsilon_{yd}$; the limiting conditions are: $\varepsilon_f = \varepsilon_{fd}$ and $\varepsilon_s = \varepsilon_{yd}$. Stress ratios are: $s'=1$, $s=1$, $1 \leq s_f \leq r \frac{0.36+\delta}{0.36}$. The neutral axis depth varies between the boundaries: $\xi = \frac{\varepsilon_{cu}(1+\delta)}{\varepsilon_{cu} + \varepsilon_{fd}}$ for $\varepsilon_f = \varepsilon_{fd}$, and $\xi = 0.636$, for $\varepsilon_s = \varepsilon_{yd}$.

The corresponding non-dimensional axial load varies between the boundaries:

$$n_{d2} = 0.8 \frac{\varepsilon_{cu}(1+\delta)}{\varepsilon_{cu} + \varepsilon_{fd}} + \mu_s(u-1) - \mu_f, \text{ for } \varepsilon_f = \varepsilon_{fd} \quad (44)$$

$$n_{d3} = 0.51 + \mu_s(u-1) - \mu_f r \frac{0.63+\delta}{0.63}, \text{ for } \varepsilon_s = \varepsilon_{yd} \quad (45)$$

The non-dimensional resisting moment varies between the boundaries:

$$m_{Rd2} = 0.8 \frac{\varepsilon_{cu}(1+\delta)}{\varepsilon_{cu} + \varepsilon_{fd}} \left[0.5(1+\delta) - 0.4 \frac{\varepsilon_{cu}(1+\delta)}{\varepsilon_{cu} + \varepsilon_{fd}} \right] + 0.5\mu_s(1-\delta)(u+1) + 0.5\mu_f(1+\delta) \quad (46)$$

$$m_{Rd3} = 0.51[0.5(1+\delta) - 0.25] + 0.5\mu_s(1-\delta)(u+1) + 0.5\mu_f(1+\delta)r \frac{0.63+\delta}{0.63}, \text{ for } \varepsilon_s = \varepsilon_{yd} \quad (47)$$

Assuming $\delta = 0$, the axial load varies between the boundaries:

$$n_{d2} = 0.8\xi_2 + \mu_s(u-1) - \mu_f, \text{ for } \varepsilon_f = \varepsilon_{fd} \quad (48)$$

$$n_{d3} = 0.51 + \mu_s(u-1) - \mu_f r, \text{ for } \varepsilon_s = \varepsilon_{yd} \quad (49)$$

The non-dimensional resisting moment varies between the boundaries:

$$m_{Rd2} \cong 0.8\xi_2 \left[\frac{1}{2} - 0.4\xi_2 \right] + \frac{1}{2}\mu_s(u+1) + \frac{1}{2}\mu_f, \text{ for } \varepsilon_f = \varepsilon_{fd} \quad (50)$$

$$m_{Rd3} \cong 0.12 + \frac{1}{2}\mu_s(u+1) - \frac{1}{2}\mu_f r, \text{ for } \varepsilon_s = \varepsilon_{yd} \quad (51)$$

All the equations developed above can be easily transformed into more treatable ones through the following coordinate shift:

$$\eta = n_{sd} + \mu_s(1-u) + \mu_f \quad (52)$$

$$\zeta = m_{Rd} - \frac{1}{2}[\mu_s(u+1) + \mu_f] \quad (53)$$

By which one can define the new boundary values for the axial load and the resisting moment at each failure mode.

Mode 1a — The variables η and ζ vary between the boundaries:

$$\eta_0 = n_{sd} + \mu_s(1-u) + \mu_f = -\mu_s u \quad (54)$$

$$\zeta_0 = m_{Rd} - \frac{1}{2}[\mu_s(u+1) + \mu_f] = -\frac{1}{2}\mu_s u \quad (55)$$

for $\varepsilon_c = 0$, and:

$$\eta_1 = \frac{2}{3}\xi_1 \quad (56)$$

$$\zeta_1 = \frac{2}{3}\xi_1 \left[\frac{1}{2} - \frac{1}{3}\xi_1 \right] \quad (57)$$

for $\varepsilon'_s = \varepsilon_{yd}$.

Applying the secant method, the resisting moment is computed from:

1078 Monti and Alessandri

$$\zeta_{(1a)}(\eta) = \frac{1}{2} \left\{ \eta_0 + \frac{\eta_1(1-\eta_1) - \eta_0}{\eta_1 - \eta_0} (\eta - \eta_0) \right\} \quad (58)$$

Mode 1b — The variables η and ζ vary between the boundaries:

$$\eta_1 = \frac{2}{3} \xi_1 \quad (59)$$

$$\zeta_1 = \frac{2}{3} \xi_1 \left[\frac{1}{2} - \frac{1}{3} \xi_1 \right] \quad (60)$$

for $\varepsilon'_s = \varepsilon_{y'd}$, and:

$$\eta_2 = 0.8 \xi_2 \quad (61)$$

$$\zeta_2 = 0.8 \xi_2 \left[\frac{1}{2} - 0.4 \xi_2 \right] \quad (62)$$

for $\varepsilon_c = \varepsilon_{cu}$.

Applying the secant method, the resisting moment is computed from:

$$\zeta_{(1b)}(\eta) = \frac{1}{2} \left\{ \eta_1 \cdot \eta_2 + [1 - (\eta_1 + \eta_2)] \eta \right\} \quad (63)$$

Mode 2 — The variables η and ζ vary between the boundaries:

$$\eta_2 = 0.8 \xi_2 \quad (64)$$

$$\zeta_2 = 0.8 \xi_2 \left[\frac{1}{2} - 0.4 \xi_2 \right] \quad (65)$$

for $\varepsilon_f = \varepsilon_{fd}$, and:

$$\eta_3 = 0.51 + \mu_f (1 - r) \quad (66)$$

$$\zeta_3 = 0.12 + \frac{1}{2} \mu_f (r - 1) \quad (67)$$

for $\varepsilon_s = \varepsilon_{y'd}$.

Applying the secant method, the resisting moment is computed from:

$$\zeta_{(2)}(\eta) = \frac{1}{2} \left\{ \eta_2(1 - \eta_2) + \frac{(0.75 - \eta_3) - \eta_2(1 - \eta_2)}{\eta_3 - \eta_2} (\eta - \eta_2) \right\} \quad (68)$$

Comparison between exact and approximate approaches

In Figure 4 a comparison is shown between the interaction diagram obtained through the exact approach and that obtained through the approximate (secant) approach. Also in this case it can be seen that the simplified equations correctly represent the interaction diagram of the FRP-strengthened section. The error committed in the approximation is around 10%, however, this is related to a case where the concrete cover is particularly thick. For lower δ , the error goes down to 5%.

DESIGN PROCEDURE FOR FRP-STRENGTHENING OF COLUMNS

Consider an existing RC column having a rectangular cross-section with base b and effective depth d , with top/bottom reinforcement ratio u , under axial load N_{sd} and bending moment M_{sd} , which does not verify the safety requirements.

In order to design the FRP strengthening, one has to select the thickness of one FRP layer $t_{f,1}$ and width b_f , based on the cross-section geometry. The elastic modulus E_f is known and the debonding strength of a single layer $f_{jdd,1}$ is then computed from relevant debonding formulas (f.e. Teng et al 2002).

Step 1. Compute the FRP-strengthening mechanical ratio, referred to the single layer:

$$\mu_{f,1} = \frac{b_f t_{f,1} f_{jdd,1}}{0.85 f_{cd} b d} \quad (69)$$

Step 2. Compute $\eta(n_{sd})$ from (52) at the given normalized value n_{sd} of the applied axial load.

Step 3. Compute the boundaries η_i , $i = 0 \dots 3$ from Table 1.

Step 4. From Table 2, through comparison of the value of $\eta(n_{sd})$ found at Step 2 with the boundaries found at Step 3, determine the relevant function for the evaluation of $\zeta_{(fm)}$ at the relevant failure mode (fm).

Step 5. Compute the FRP-strengthened moment capacity from:

$$m_{Rd}(n_{sd}) = \zeta_{(fm)}(\eta) + \frac{1}{2} [\mu_s(u+1) + \mu_f] \quad (70)$$

Step 6. Compare with the acting normalized bending moment m_{sd} , in order to verify that:

$$m_{Rd}(n_{sd}) \geq m_{sd} \quad (71)$$

If the verification is not satisfied, the number of FRP layers should be increased to n_f and the process should be repeated from Step 2, with the updated FRP-strengthening mechanical ratio μ_f , given by (because $f_{jdd,n_f} = f_{jdd,1} \sqrt{n_f}$):

$$\mu_f = \mu_{f,1} \cdot \sqrt{n_f} \quad (72)$$

CONCLUSIONS

A study has been presented that proposes an approach to design the amount of FRP to strengthen RC columns sections with insufficient bending capacity. The method accounts for the interaction between bending and axial load. Two approaches are compared: an exact one vs. an approximate one, which makes use of a secant method. The resulting interaction diagram obtained with the latter shows very little deviation from the exact one, with the significant advantage of using extremely simple equations for the different failure modes. The proposed method lends itself to a straightforward design of FRP strengthening of under-designed concrete columns: starting from the assigned axial load, the failure mode is directly found and the corresponding moment capacity computed. It has been shown that the failure mode depends on the amount of both the existing steel reinforcement and the added FRP strengthening and that the failure mode can be modified by adjusting the amount of the latter.

NOTATION

The following symbols are used in this paper:

A_f	area of FRP strengthening
A_s	cross sectional area of tensile steel reinforcement
A'_s	cross sectional area of compressive steel reinforcement
E_f	elastic modulus of FRP strengthening
b	width of cross – section
b_f	width of FRP strengthening
d	effective depth of cross – section
d'	concrete cover thickness
f_{cd}	design value of concrete cylinder compressive strength
f_{fd}	design value of FRP strengthening debonding strength
$f_{fd,1}$	design value debonding strength of a single layer of FRP strengthening
$f_{fd,nf}$	design value debonding strength of a n_f layers of FRP strengthening
f_{yd}	design yield strength of reinforcement
x	neutral axis depth
k	distance of resultant of the concrete compressive stress from the extreme fibre
m_{Rd}	non-dimensional value of resisting moment M_{Rd}
M_{Rd}	resisting bending moment
m_{Rd0}	non-dimensional resisting moment lower boundary for failure mode 1a
m_{Rd1}	non-dimensional resisting moment boundary between failure mode 1a and 1b
m_{Rd2}	non-dimensional resisting moment boundary between failure mode 1b and 2
m_{Rd3}	non-dimensional resisting moment boundary between failure mode 2 and 3
m_{Rd4}	non-dimensional resisting moment boundary between failure mode 3 and 4
$m_{Rd(nf)}$	non-dimensional resisting moment in relevant failure mode nf
n_{d0}	non-dimensional axial load lower boundary for failure mode 1a
n_{d1}	non-dimensional axial load boundary between failure mode 1a and 1b
n_{d2}	non-dimensional axial load boundary between failure mode 1b and 2
n_{d3}	non-dimensional axial load boundary between failure mode 2 and 3

n_{d4}	non-dimensional axial load boundary between failure mode 3 and 4
n_f	number of FRP layers
n_{sd}	non-dimensional values of the applied axial load N_{sd}
N_{sd}	design value of the applied axial force
r	parameter
s	tensile steel reinforcement stress ratio
s'	compressive steel reinforcement stress ratio
s_f	FRP stress ratio
t_f	thickness of FRP
$t_{f,1}$	thickness of one FRP layer
u	compressive/tensile steel reinforcement ratio
α	factor defining the equivalent concrete stress block
δ	cover ratio
ϵ_c	compression strain in concrete
ϵ_{cu}	concrete ultimate strain
ϵ_f	FRP tensile strain ϵ_f
ϵ_{fd}	FRP ultimate strain
ϵ_{yd}	yield strain of steel reinforcement
ϵ_s	strain in tension steel reinforcement
ϵ'_s	strain in compression steel reinforcement
ϵ_{su}	ultimate strain of steel reinforcement
η	variable for coordinate shift
η_1	variable η lower boundary for failure mode 1a
η_2	variable η boundary between failure mode 1a and 1b
η_3	variable η boundary between failure mode 1b and 2
$\eta(n_{sd})$	η value for non-dimensional applied axial load n_{sd}
$\mu_{f,1}$	single layer FRP-strengthening mechanical ratio
μ_f	FRP-strengthening mechanical ratio
μ_s	tensile steel reinforcement mechanical ratio
ξ	non-dimensional neutral axis depth
ξ_1	parameter
ξ_2	parameter
σ_f	tension in FRP-strengthening
σ_s	tension in tensile steel reinforcement
σ'_s	tension in compressive steel reinforcement
ζ	variable for coordinate shift
ζ_1	variable ζ lower boundary for failure mode 1a
ζ_2	variable ζ boundary between failure mode 1a and 1b
ζ_3	variable ζ boundary between failure mode 1b and 2
$\zeta_{(fm)}(\eta)$	ζ value at the relevant failure mode (fm).

REFERENCES

Teng J.G., Chen J.S., Smith S.T., Lam (2002) “FRP Strengthened RC Structures”. *John Wiley and Sons*. Ltd. Chirchester, England

Table 1. Boundaries for the normalized axial load η , where: $\xi_1 = r/(r+1)$ and $\xi_2 = 1.75r/(1.75r+1)$, with $r = 2/1000\varepsilon_{fd}$.

i	η_i
0	$-\mu_s u$
1	$\frac{2}{3}\xi_1$
2	$0.8\xi_2$
3	$0.51 + \mu_f(1-r)$

Table 2. Equations defining the normalized bending capacity between the boundaries defined in Table 1.

Failure mode	η_i	$\zeta_{(fm)}(\eta)$
1a	$\eta_0 \leq \eta \leq \eta_1$	$\zeta_{(1a)}(\eta) = \frac{1}{2} \left\{ \eta_0 + \frac{\eta_1(1-\eta_1) - \eta_0(\eta - \eta_0)}{\eta_1 - \eta_0} \right\}$
1b	$\eta_1 \leq \eta \leq \eta_2$	$\zeta_{(1b)}(\eta) = \frac{1}{2} \left\{ \eta_1 \cdot \eta_2 + [1 - (\eta_1 + \eta_2)]\eta \right\}$
2	$\eta_2 \leq \eta \leq \eta_3$	$\zeta_{(2)}(\eta) = \frac{1}{2} \left\{ \eta_2(1-\eta_2) + \frac{(0.75 - \eta_3) - \eta_2(1-\eta_2)}{\eta_3 - \eta_2} (\eta - \eta_2) \right\}$

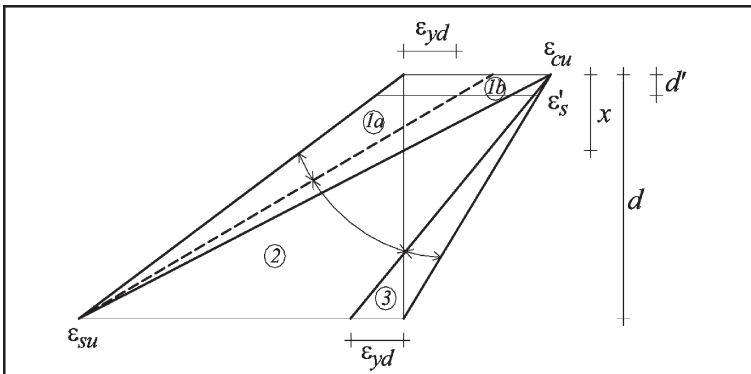


Figure 1 — Failure modes of an unstrengthened RC section.

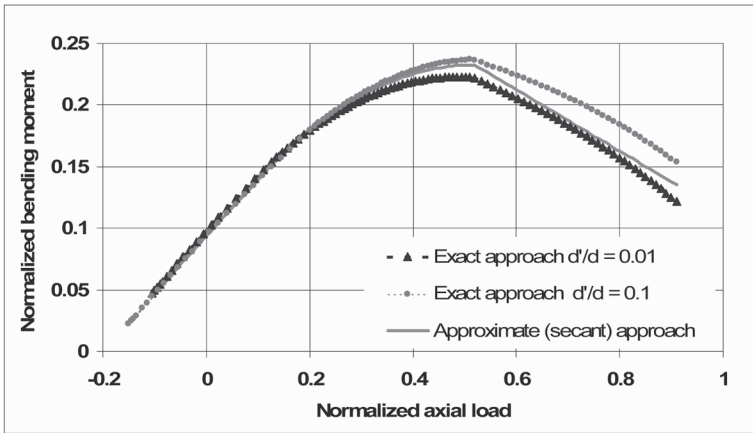


Figure 2 — Comparison between exact and approximate approaches for an unstrengthened RC section under combined bending and axial load.

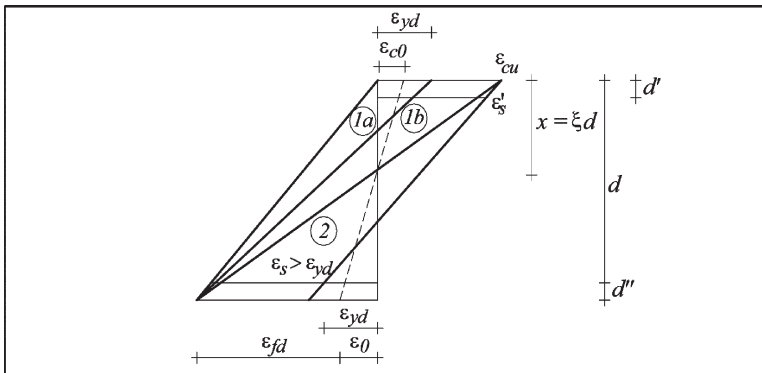


Figure 3 — Failure modes of an FRP-strengthened RC section.

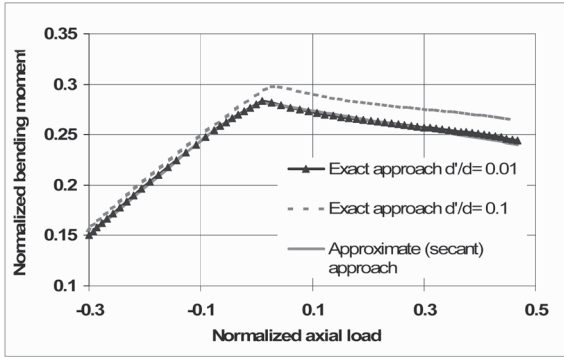


Figure 4 — Comparison between exact and approximate approaches for an FRP-strengthened RC section under combined bending and axial load.